Jurnal Kejuruteraan 34(5) 2022: 851-860
https://doi.org/10.17576/jkukm-2022-34(5)-12

Green Extraction Method of Cellulose Fibers from Oil Palm Empty Fruit Bunches

Maha Mohammad Al-Rajabi[a] & Teow Yeit Haan[a, b*]

[a]*Department of Chemical and Process Engineering,*
[b]*Research Centre for Sustainable Process Technology (CESPRO), Faculty of Engineering and Built Environment, Universiti Kebangsaan Malaysia, 43600 Bangi, Selangor Darul Ehsan, Malaysia.*

**Corresponding author: yh_teow@ukm.edu.my*

Received 17 July 2021, Received in revised form 01 December 2021
Accepted 31 December 2021, Available online 30 September 2022

ABSTRACT

Oil palm empty fruit bunches (OPEFB) is one of the major biomass wastes produced from palm oil extraction process. Due to high cellulose content in OPEFB, the cellulose fibers in OPEFB can be extracted and utilized in versatile applications as a sustainable process technology development. Among multiple pre-treatment processes, chemical pre-treatment is most efficient for the removal of hemicellulose and lignin in extracting high purity cellulose from lignocellulosic biomass. With the undisputed importance of green technology for the progress of our society, it is vital to engage and leverage on green technology in chemical pre-treatment method for extracting cellulose from OPEFB. The objective of this study is to explore a green extraction method for cellulose from OPEFB using low concentration and eco-friendly chemicals. Fourier transform infrared spectroscopy and field emission scanning electron microscope was used to detect the functional groups and to observe the surface morphology of OPEFB, de-waxed OPEFB fibers, delignified OPEFB fibers, acid hydrolyzed OPEFB fibers, and OPEFB extracted cellulose fibers at different stages in confirming the removal of wax, lignin, and hemicellulose from OPEFB extracted cellulose at the end of the extraction process. Crystallinity index increased from 28% for OPEFB to 72% for the OPEFB extracted cellulose, affirms the degradation of OPEFB's amorphous structure and transforms into higher crystallinity structure. This work has successfully developed a green extraction method for OPEFB cellulose fibers as part of sustainable process technology which would promote the utilization of lignocellulosic agricultural waste from palm oil industry in various applications.

Keywords: Cellulose; Chemical pre-treatment; Extraction; Green technology, Oil palm empty fruit bunches (OPEFB)

INTRODUCTION

The increase of palm oil demand contributes to the rapid development of palm oil industry in Malaysia. Malaysia has produced 19.14 million tonnes of palm oil annually, with oil palm plantation area of 5.865 million hectares in 2020(Nordin et al. 2021). This has directly resulted an increase of biomass waste production along with the palm oil extraction process (Haan et al. 2018). One of the major biomass waste produced from palm oil extraction process is oil palm empty fruit bunches (OPEFB). Malaysia is estimated in producing around 7.78 million tonnes of OPEFB annually (Hamzah et al. 2019). Typically, OPEFB is burned as low heating value solid fuel in boiler and its ash is used as fertilizer. However, burning would impose serious air pollution problem and Department of Environment (DOE) Malaysia regulations had raised the awareness of stakeholders on palm oil industry waste management. Recently, many research are focusing on green technology and sustainability process innovation, focusing on the utilization of biomass waste as resources for valuable products (Haan et al. 2020; Pangsang et al. 2019).

Lignocellulosic biomass OPEFB consists of 37.3 – 46.5% cellulose, 25.3 – 33.8% hemicellulose, and 27.6 – 32.5% lignin (Sudiyani et al. 2013).With high cellulose content in OPEFB, the cellulose fibers in OPEFB can be extracted and utilized in versatile applications such as the synthesis of cellulose hydrogel in biomedical application (AL-Rajabi & Haan 2021; Salleh et al. 2019), an adsorbent in water and wastewater treatment (Thoe et al. 2019), a reinforcing agent in composite materials (Khalid et al. 2009), an energy storage materials like super capacitors and lithium ion battery (Faizi et al. 2017), an emulsion stabilizer due to its remarkable emulsifying performance (Li et al. 2019). Cellulose fibers in lignocellulosic materials are ordered, tightly packed, and embedded in a matrix of hemicelluloses and lignin. Thus, series of pre-treatment processes is needed to break down the lignocellulosic materials recalcitrance for the extraction of cellulose fibers (Isroi et al. 2012; Yin et al. 2021). Multiple pre-treatment processes of lignocellulosic materials had been developed such as physical pre-treatment (e.g: microwave irradiation) (Nair 2017), thermo-physical pre-treatment (e.g: steam explosion) (Yang et al. 2018), chemical pre-treatment (e.g:

organic solvent) (Nazir et al. 2013), thermochemical pre-treatment (e.g: ammonia fiber explosion) (Kim 2018), and biological pre-treatment (Putro et al. 2016).

Each pre-treatment process has its own advantages and disadvantages. Selection of pre-treatment process depends on several factors, for instance, economical assessment, composition of lignocellulosic biomass, and environmental impact (Harmsen et al. 2010). As an example, physical pre-treatment is eco-friendly and producing less toxic by-products, however, it is high energy consuming process (Baruah et al. 2018). On the other hand, although ammonia fiber explosion, a thermochemical pre-treatment is efficient in removing lignin, it is only efficient for lower lignin lignocellulosic materials (Kim 2018). In addition, even that microorganisms in biological pre-treatment can degrade lignin effectively, biological pre-treatment is the most expensive pre-treatment method due to the high cost of certain microorganisms (Putro et al. 2016). Whereas, chemical pre-treatment is most efficient for the removal of hemicellulose and lignin in extracting high purity cellulose from lignocellulosic biomass (Motaung & Mtibe 2015; Putro et al. 2016). Moreover, it is cost competitive compared to physical and biological pre-treatment processes (Brodeur et al. 2011) as it involves simple reactors and its ease of operation (Bensah & Mensah 2013).

Among chemical treatment methods, chemical treatment with the use of organic solvents is preferable as organic solvents are less corrosive and easy to control at low operating temperature and pressure (Nazir et al. 2013). Hence, chemical treatment with the use of organic solvents is considered as green method and claimed as more eco-friendly (Ling Hii et al. 2014; Nazir et al. 2013). Among numerous organic solvents, formic acid has shown great potential for extensive delignification with simultaneous removal of hemicellulose and good retention of cellulose (Yu et al. 2013; Yu et al. 2018). Besides, formic acid pre-treatment is considered as environmental friendly as the formic acid can be recycled and reused through distillation process (G. Yu et al. 2013; Zhang et al. 2016). With the undisputed importance of green technology for the progress of our society, it is vital to engage and leverage green technology in chemical method for extracting cellulose from OPEFB. Nazir et al. (2013) had developed an eco-friendly cellulose extraction method for extracting cellulose from OPEFB. It was conducted by high energy steam sodium hydroxide treatment followed by formic acid treatment. High cellulose content (93.7%) with high crystallinity (69.9%) obtained in Nazir et al. (2013) study confirmed the efficiency of the developed eco-friendly cellulose extraction method (Nazir et al. 2013).

Although the extraction of cellulose from OPEFB using environmentally friendly organic solvent such as formic acid in chemical pre-treatment has been explored, there is still a need for further improve this chemical pre-treatment method towards a greener process, possibly by not using high energy steam treatment and decrease in used chemical concentration and/or amount along the chemical pre-treatment method while maintaining high purity of the extracted cellulose. The present study employed ethanol as the green solvent in de-waxing process for the removal of non-structural components, nitrogenous compounds, inorganic compounds, and waxes from OPEFB (Rosli et al. 2017) by replacing conventional solvents such as toluene, methanol, and benzene. Hence, this process could be considered as an eco-friendly extraction method (Fahma et al. 2010; Visakh & Morlanes 2016). Following the same concept, delignification stage was performed using 3 w/v% sodium hydroxide. By this, less solvent and lower concentration in comparison with Nazir et al. (2013) study, where they used mixture of 10% sodium hydroxide and 10% hydrogen peroxide during delignification stage. Also, using 3 w/v% sodium hydroxide in delignification stage will replace toxic sodium chlorite treatment which is widely used as a standard reagent for the delignification (Park et al. 2015). Therefore, the objective of this study is to explore a green extraction method for cellulose from OPEFB using low concentration and eco-friendly chemicals. Green extraction method of cellulose from OPEFB is part of sustainable process technology which would promote the utilization of lignocellulosic agricultural waste from palm oil industry in various applications.

METHODOLOGY

MATERIALS

OPEFB was collected from Tennamaram palm oil mill located at Bestari Jaya, Selangor Darul Ehsan, Malaysia. The OPEFB was stored in cold room at 4 ^{o}C to avoid the growth of fungi before use. Formic acid (98-100 w/w%) was purchased from Thermo Fisher Scientific, USA. Sodium hydroxide (NaOH) and hydrogen peroxide (30 w/w%) were obtained from Classic Chemicals Sdn. Bhd., Malaysia. On the other hand, ethanol (99.5 v/v%) was purchased from Scienfield Expertise PLT, Malaysia. All chemicals were ACS grade and used as purchased.

Extraction of Cellulose from OPEFB

The cellulose extraction process was adapted and modified from a research study conducted by Nazir et al. (2013). Firstly, OPEFB was washed several times with 1 w/v% detergent until the rinse water turned into colorless. Next, washed OPEFB was dried in an oven at 100 ± 2 ^{o}C until constant weight was obtained. Following, dried OPEFB was cut into 1-3 cm length, and sieved with stainless steel sieve at 1.18 mm opening mesh. Dry OPEFB was de-waxed using 70 v/v% ethanol, at OPEFB/ethanol weight to volume (w/v) ratio of 1:20 in soxhlet extraction apparatus for 6 hours at 78 ± 2 ^{o}C without stirring. The OPEFB fibers were then collected and washed with plenty deionized (DI) water to remove ethanol traces before further dry in an oven at 100 ± 2 ^{o}C until constant weight was obtained.

Delignification stage was started by adding 3 w/v% NaOH solution to de-waxed OPEFB fibers at solid/liquid w/v ratio of 1:9. The mixture was then heated to 121 °C using an oil bath for 1 hour. Next, dark brown supernatant after the completion of delignification process was separated from OPEFB fibers. The delignified OPEFB fibers was washed several times until the rinse water turned into colorless (Huang et al. 2017). Acid treatment was then started following delignification stage. 10 g of delignified OPEFB fibers were soaked in 200 mL mixture of 20 v/v% formic acid and 10 v/v% hydrogen peroxide at volume/volume ratio (v/v) of 1:1. The mixture was heated to 85 °C in water bath for 2 hours. The acid hydrolyzed OPEFB fibers were then collected from vacuum filtration and washed several times with DI water until neutral pH was obtained at supernatant.

Finally, the extracted light yellow cellulose fibers after acid treatment process were bleached by suspending in 10 v/v% hydrogen peroxide at 60 °C for 90 minutes. The pH of 10 v/v% hydrogen peroxide was adjusted to pH 9 using 10 w/v% NaOH (Nazir et al. 2013). Next, white cellulose fibers were vacuum filtered, it was rinsed several times with DI water until neutral pH was obtained at supernatant. The insoluble fraction of cellulose fibers was collected, dried in an oven at 60 ± 2 °C for 24 hours and weighed. Dry weight yield of extracted cellulose fibers was calculated using Equation (1).

Dry weight yield of extracted cellulose fibers

$$(w/w)\% = \left[\frac{W_C}{W_R}\right] x100\% \quad (1)$$

Where W_C is the weight of dry extracted cellulose fibers and W_R is the weight of OPEFB.

CHARACTERIZATION OF OPEFB EXTRACTED CELLULOSE

Functional Groups

Fourier transform infrared spectroscopy (FTIR), Nicolet 6700 (Thermo Scientific, US) was used to detect the functional groups presence on OPEFB, de-waxed OPEFB fibers, delignified OPEFB fibers, acid hydrolyzed OPEFB fibers, and OPEFB extracted cellulose fibers at attenuated total reflectance (ATR) mode for wavenumber ranging from 500 to 4000 cm^{-1} and 32 scans.

Surface Morphology and Structure

The surface morphology and structure of OPEFB, de-waxed OPEFB fibers, delignified OPEFB fibers, acid hydrolyzed OPEFB fibers, and OPEFB extracted cellulose fibers were observed using field emission scanning electron microscope (FESEM), Merlin Compact (Carl Zeiss, Germany). The samples were coated with a thin layer of gold using vacuum sputter coater, Q150R (Quorum Technologies, England) prior FESEM analysis to reduce the charging effect. Next, the samples were mounted onto the sample holder using the carbon tape and observed under 100× and 500× magnification.

Crystallinity

The crystalline property of OPEFB and OPEFB extracted cellulose fibers was analyzed using X-ray diffraction (XRD), D8 Advance X-ray diffractometer (Bruker AXS, Germany). D8 Advance X-ray diffractometer was equipped with CuKα radiation source (1.5406 Å) and 1-D fast detector (Lynx-Eye) operated at 40 kV and 40 mA. The XRD micrographs were obtained at 2θ scan range of 5° to 80° and step size of 0.025° with the exposure rate of 0.1 s per step. Crystallinity index (CI) of the samples was calculated by peak height method introduced by Segal et al. (1959) as presented in Equation (2).

$$CI\ (\%) = \left[\left(1 - \frac{I_{am}}{I_{002}}\right)\right] x100\% \quad (2)$$

Where I_{002} is the highest peak intensity of the crystalline fraction and I_{am} is the lowest peak intensity of the amorphous region.

The crystallite size (D) of OPEFB and OPEFB extracted cellulose fibers was determined using Scherrer's equation as presented in Equation (3) (Patterson 1939).

$$D = \frac{K\lambda}{\beta \cos \theta} \quad (3)$$

Where K is the constant (0.91), λ is the X-ray wavelength (nm), θ is the Bragg's angle (°), and β is the full width at half maximum (FWHM) intensity of the peak at diffraction plane 002 (radians).

RESULTS AND DISCUSSION

CHARACTERIZATION OF OPEFB EXTRACTED CELLULOSE

Functional Groups

Figure 1 shows the FTIR spectrum of OPEFB, de-waxed OPEFB fibers, delignified OPEFB fibers, acid hydrolyzed OPEFB fibers, and OPEFB extracted cellulose fibers. These FTIR spectrum presented different stages in OPEFB cellulose extraction process, including washing, de-waxing, delignification, acid hydrolysis, and lastly bleaching. As presented in Figure 1, the FTIR spectrum of OPEFB, de-waxed OPEFB fibers, delignified OPEFB fibers, acid hydrolyzed OPEFB fibers, and OPEFB extracted cellulose fibers is having a broad peak ranging from 3375 to 3409 cm^{-1}, confirmed the presence of hydroxyl (O─H) stretching vibration (Nazir et al. 2013). The OPEFB extracted cellulose fibers is having O-H stretching vibration peak at peak intensity higher than that of OPEFB. According to

transmittance readings in Figure 1, the increment of O─H stretching vibration peak was 43.18% in OPEFB extracted cellulose in comparison to OPEFB fibers. The removal of hemicelluloses, lignin, waxes, and impurities from OPEFB surface exposes the cellulose content in OPEFB structure, and reflected to reactive O-H functional group in FTIR spectrum (Ibrahim et al. 2019). It is therefore contributing to higher peak intensity for OPEFB extracted cellulose fibers. Unfortunately, the O-H stretching vibration peak intensity slightly decrease after the bleaching process, probably due to a slight declination of cellulose content by hydrogen peroxide treatment. On the other hand, the peak exists at 2918 cm^{-1} is attributed by asymmetric $─CH_2$ stretching from waxes (Djajadi et al. 2017) while the peak exists at 2902 cm^{-1} is ascribed to CH and CH_2 stretching vibration in cellulose (Parida et al. 2015; Qu et al. 2014). The peak appeared at 2918 cm^{-1} in OPEFB disappeared while a peak appeared at 2902 cm^{-1} after de-waxing process, indicating the successful removal of waxes after de-waxing stage.

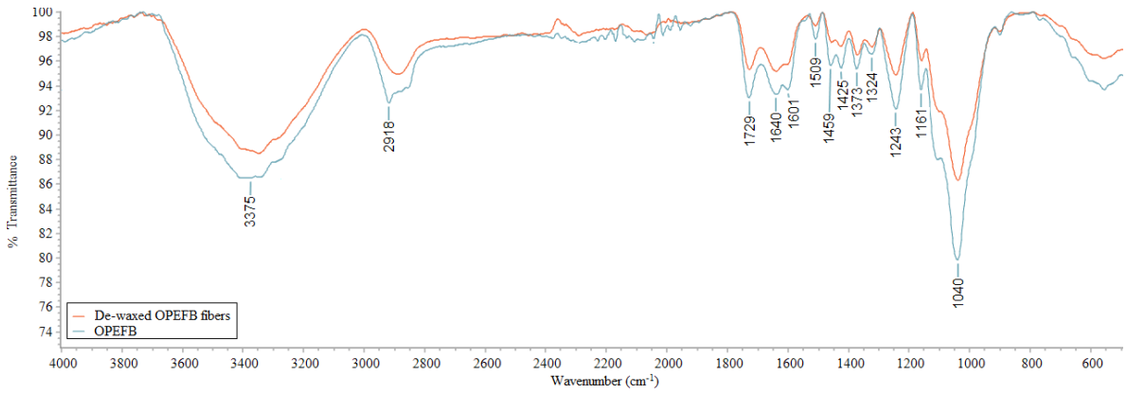

(a)

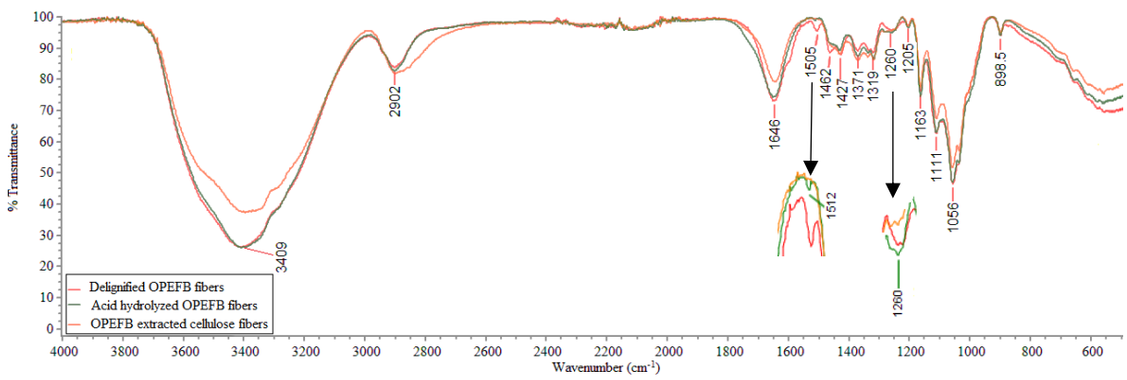

(b)

FIGURE 1. FTIR spectrum of (a) OPEFB and de-waxed OPEFB fibers, (b) delignified OPEFB fibers, acid hydrolyzed OPEFB fibers, and OPEFB extracted cellulose fibers

A sharp peak at 1729 cm^{-1} refers to C=O stretching vibration of carboxylic acid and ester components (Wang et al. 2019). The existence of this peak in OPEFB indicates for the presence of hemicelluloses. However, the intensity of C=O stretching vibration is decreased after de-waxing process and disappeared following de-lignification process due to the complete dissolution of hemicellulose carboxyl and acetyl groups in NaOH solution (Khenblouche et al. 2019). Besides, the peak located between 1640 and 1646 cm^{-1} is attributed to the O─H bending (Teow et al. 2018). The increasing of O-H bending peak intensity after delignification process reflects the removal of lignin as lignin has lower water absorption capability (Tanpichai et al. 2019). The interaction between delignified OPEFB fibers and water molecules is therefore stronger after the removal of hydrophobic lignin from OPEFB (Tanpichai et al. 2019). Characteristic peak at 1601 cm^{-1} refers to C–O stretching in an aromatic ring of the lignin (Tsamo et al. 2019). This peak is only observed in OPEFB's FTIR spectrum. It is almost completely reduced after de-waxing process and disappeared for the afterward processes, illustrating that de-waxing process had removed most of the soluble lignin and it was completely removed after delignification process. During delignification process, ester bonds linking the lignin to the hemicellulose in lignin-carbohydrate network are disrupted, where lignin components become solubilized and could be removed from OPEFB (Modenbach & Nokes 2014). On top of that, the characteristic peaks at 1509,

1505, and 1512 cm^{-1} are associated to the aromatic skeletal vibration (Rashid et al. 2016), at 1459 and 1462 cm^{-1} are relates to C–H deformations (Wang et al. 2017), and at 1243 cm^{-1} indicates the presence of C-O-C stretching of aryl-alkyl ether (Nazir et al. 2013) in lignin. These peaks intensity is gradually decreased along OPEFB cellulose extraction process and disappeared at the end of the process indicates the complete removal of lignin from OPEFB.

Moreover, characteristic peaks located at 1425 to 1427 cm^{-1}, 1373 and 1371 cm^{-1}, and 1324 and 1319 cm^{-1} are due to the presence of $-CH_2$ bending vibration (Hospodarova et al. 2018), C–H bending vibration (Baharin et al. 2018), and C-O bending vibration (Gonultas & Candan 2018), respectively. These peaks exist in all FTIR spectrum in Figure 1, represent the presence of carbohydrate cellulose, and hemicellulose (Gonultas & Candan 2018; Isroi et al. 2012). The intensity of these characteristic peaks increased after delignification process as the cellulose content was increased after significant removal of hemicelluloses and lignin from OPEFB. Likewise, the characteristic peaks around 1161 to 1163 cm^{-1}, 1107 to 1111 cm^{-1}, and 1040 to 1056 cm^{-1} are attributed to C-O asymmetric stretching, C–OH skeletal vibration, and C-O-C pyranose ring skeletal vibration, respectively (Wang et al. 2017). These characteristic peaks associated to the presence of cellulose in samples. Similarly, the intensity of these characteristic peaks is increased after delignification process, confirmed the removal of lignin and hemicellulose, thus leading to an increase of cellulose content. In short, it is evident that the OPEFB cellulose fibers has been successful extracted from a series of pre-treatment processes for the removal of hemicelluloses, lignin, pectins, and waxes in obtaining OPEFB cellulose fibers with high purity.

Surface Morphology and Structure

FESEM micrographs in FIGURE 2 show the surface morphology of OPEFB, de-waxed OPEFB fibers, delignified OPEFB fibers, acid hydrolyzed OPEFB fibers, and OPEFB extracted cellulose fibers. As presented in Figure 2, the surface of OPEFB is rough, covered with impurities such as the circular shape silica bodies, wax, and inorganic metals as agreed by Rosli et al. (2017). This could be further explained by the microstructure and cell wall structure of OPEFB illustrated in Figure 3. As illustrated in Figure 3, OPEFB consists of solid protective layer, mainly lignin and hemicellulose to prevent water loss from the plant surface (Rosli et al. 2017). The cellulose fibers are embedded inside the solid protective layer. After de-waxing process, pinholes were appeared on the surface of de-waxed OPEFB fibers with 'rotten' like appearance. This is possibly due to the removal of silica bodies, impurities, and partial removal of lignin and hemicellulose from OPEFB as supported by FTIR spectrum in Figure 1 (Qu et al. 2014). With the surface fracture created from de-waxing process, the surface of de-waxed OPEFB fibers look rougher than that of OPEFB.

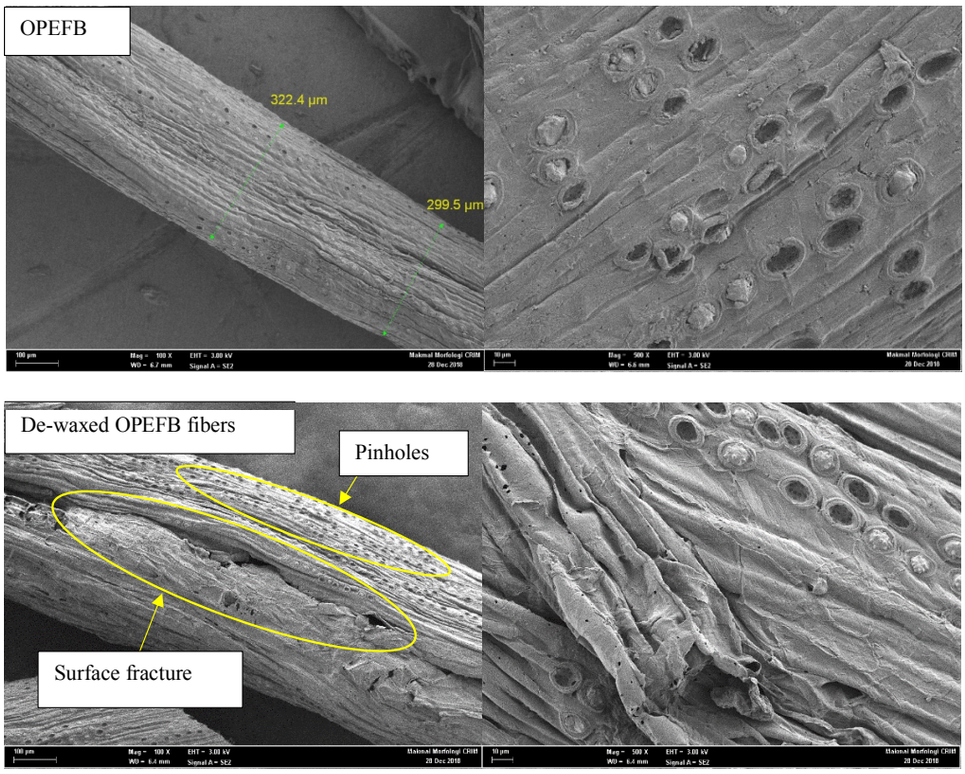

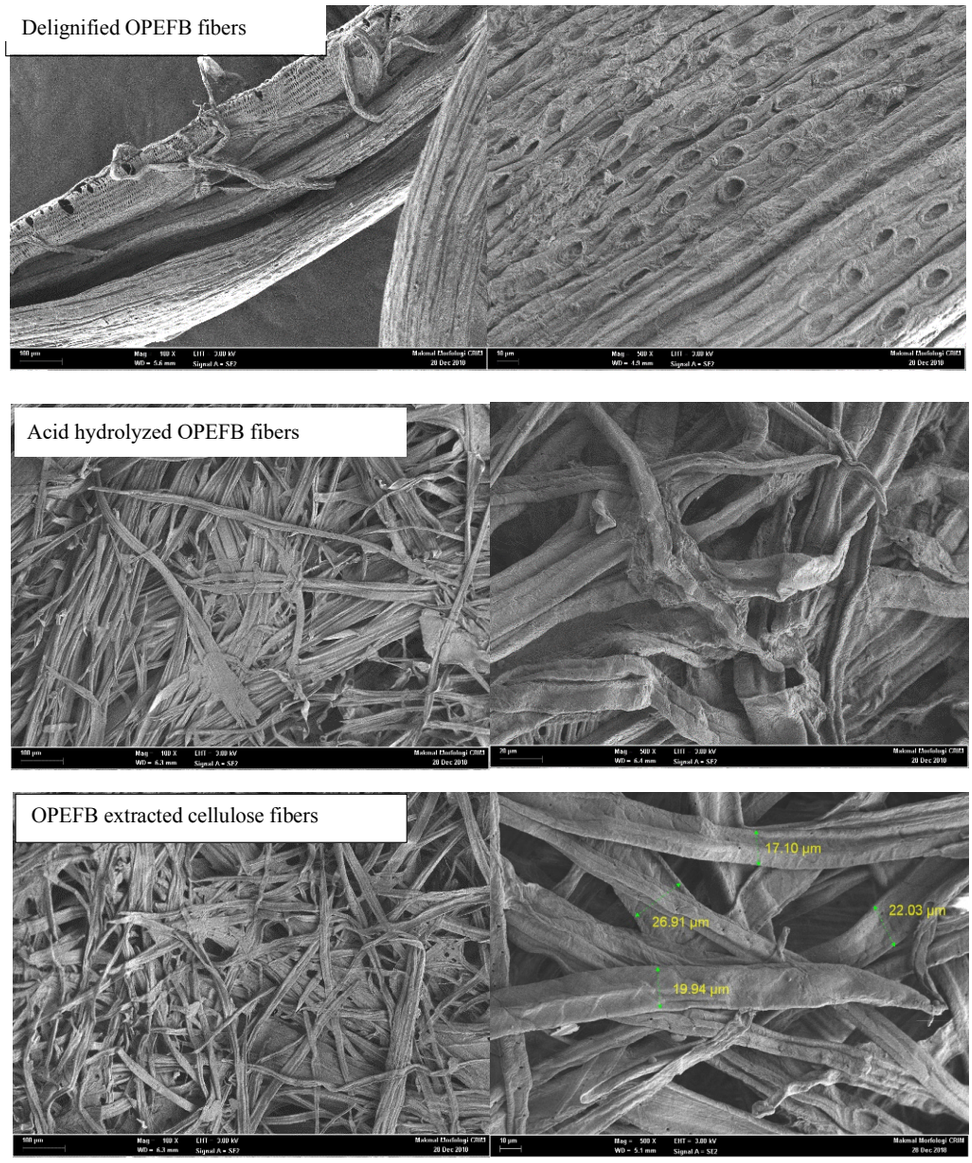

FIGURE 2. FESEM micrographs of OPEFB, de-waxed OPEFB fibers, delignified OPEFB fibers, acid hydrolyzed OPEFB fibers, and OPEFB extracted cellulose fibers at the magnification of (a) 100× and (b) 500×

As most of the impurities were removed during the delignification process, delignified OPEFB fibers show even rougher and corrugated surface with large number of holes and pits. Fatty deposits or 'tyloses' hidden below the surface of de-waxed OPEFB fibers were removed through delignification process (Chieng et al. 2017). Besides, solid-cell structure of de-waxed OPEFB fibers was destructed with the removal of hemicellulose and lignin from de-waxed fibers' surface. Hence, as depicted in FESEM micrograph, delignified OPEFB fibers depicted network with more cylindrical holes. Delignification process broken the lignocellosic complex and dissolved the lignin and hemicellulose to expose the hidden cellulose to the surface.

On the other hand, isolated fibril is shown on acid hydrolyzed OPEFB fibers. This observation is notified due to the removal of cementing wax, hemicellulose, and most of the lignin from fibers' surface. With the removal of residual lignin fraction, acid hydrolyzed OPEFB fibers surface is rough and not flat (Chowdhury et al. 2019). Comparatively, the surface of OPEFB extracted cellulose fibers is clean, smooth, and free of deposition of debris. Furthermore, the individual fibers of OPEFB extracted cellulose shows a decrease in diameter. The diameter of OPEFB was reduced from 228.05±20.22 µm to 24.26±2.33 µm after the completion of cellulose extraction process due to the removal of outer solid layer components including hemicelluloses, lignin, pectins, and waxes. The calculated dry weight yield of OPEFB extracted cellulose fibers is 34.87 ± 3.23%, which is proximity to the yield value of 20-43% reported in literature (Sisak et al. 2015; Wanrosli et al. 2004). Consequently, it can be concluded that the eco-friendly extraction method is able to extract cellulose from OPEFB with high purity and high yield value.

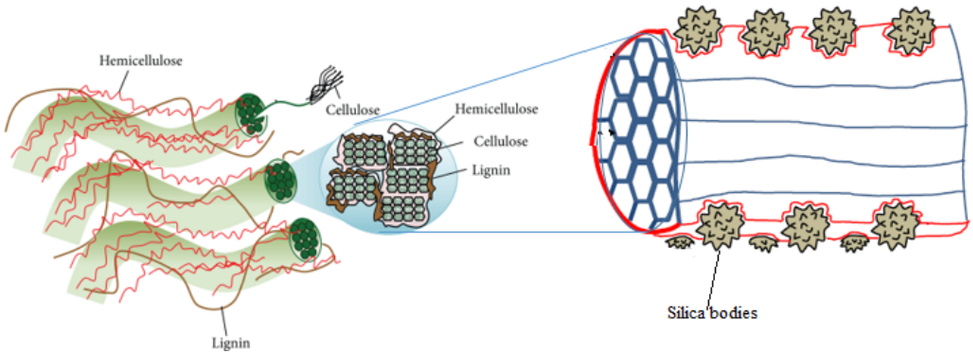

FIGURE 3. Microstructure and cell wall structure of OPEFB (Omar et al. 2014; Yahya et al. 2015)

Crystallinity

Figure 4 shows the XRD diffractograms of OPEFB and the OPEFB extracted cellulose fibers. Two well-defined characteristic peaks are revealed at 2θ =14.5° and 2θ =21.8°, representing the amorphous structure and crystalline structure, respectively (Ching & Ng 2014). The amorphous structure of OPEFB and OPEFB extracted cellulose fibers is due to the presence of lignin and hemicelluloses; whereas the crystalline structure is mainly attributed by cellulose (Martelli-Tosi et al. 2017). The decrease of peak intensity at 14.5° and the increase of peak intensity at 21.8° for OPEFB extracted cellulose fibers signifies the transformation of OPEFB nature from amorphous to crystalline. This XRD diffractograms supports FTIR and FESEM analysis on the removal of amorphous hemicelluloses and lignin for the extraction of cellulose from OPEFB.

Table 1 shows the CI and crystallite size of OPEFB and OPEFB extracted cellulose fibers. As presented in Table 1, CI of OPEFB is 28% whereas the CI for OPEFB extracted cellulose fibers is 72%. CI increases significantly after a series of treatment processes, confirms the degradation of OPEFB's amorphous structure and transforms into higher crystallinity structure (Haan et al. 2020). On top of that, the CI value of 72% for OPEFB extracted cellulose fibers is found to be in proximity to the CI value of 65.72–70% in literature (Haan et al. 2020; Nazir et al. 2013). Comparative CI value with literature supports the successful extraction of cellulose fibers from OPEFB in this study. On the other hand, the crystallite size of OPEFB is calculated as 5.1 nm and the crystallite size for OPEFB extracted cellulose fibers is 3.3 nm. Decreasing in crystallite size for OPEFB extracted cellulose fibers is probably attributed to the removal of amorphous domains on OPEFB surface, hence leading to smaller cellulose crystallites. Similar finding was also obtained by Khenblouche et al. (2019) where 3.62 nm crystallite size extracted cellulose was obtained from retama raetam stems plant.

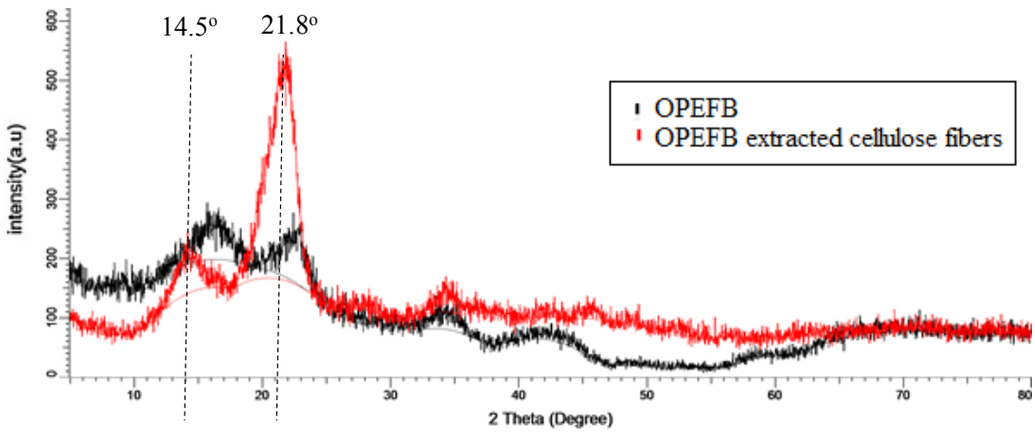

FIGURE 4. XRD diffractogram of OPEFB and OPEFB extracted cellulose fibers

TABLE 1. CI and crystallite size of OPEFB and OPEFB extracted cellulose fibers

Material	CI (%)	Crystallite size, D (nm)
OPEFB	28	5.1
OPEFB extracted cellulose fibers	72	3.3

CONCLUSION

In conclusion, this study had successfully explored a green extraction method for cellulose from OPEFB using low concentration and eco-friendly chemicals. Both FITR and FESEM analysis confirmed the successful extraction of OPEFB cellulose fibers from a series of pre-treatment processes for the removal of hemicelluloses, lignin, pectins, and waxes. The diameter of OPEFB was decreased from 228.05±20.22 μm to 24.26±2.33 μm at the end of the extraction process. On the other hand, its CI was increased from 28% for OPEFB to 72% for OPEFB extracted cellulose fibers attributed to the removal of amorphous hemicelluloses and lignin from OPEFB. Green extraction method of cellulose from OPEFB with high purity and high yield (34.87 ± 3.23%) is established in this study which would promote the utilization of lignocellulosic agricultural waste from palm oil industry in various applications.

ACKNOWLEDGEMENTS

The authors wish to gratefully acknowledge the funding for this work by Dana Modal Insan (MI-2019-017) and Geran Universiti Penyelidikan (GUP-2017-098). The authors also wish to acknowledge Centre for Research and Instrumentation Management (CRIM), UKM for XRD and FESEM analysis.

DECLARATION OF COMPETING INTEREST

None

REFERENCES

AL-Rajabi, M. M. & Haan, T. Y. 2021. Green synthesis of thermo-responsive hydrogel from oil palm empty fruit bunches cellulose for sustained drug delivery. *Polymers* 13(2153).

Baharin, K. W., ZaKaria, S., Ellis, amanda V., Talip, N., Kaco, H., Gan, S., Zailan, F. diyana, et al. 2018. Factors affecting cellulose dissolution of oil palm empty fruit bunch and kenaf pulp in NaOH / urea solvent. *Sains Malaysiana* 47(2): 377–386. doi:10.17576/jsm-2018-4702-20

Baruah, J., Nath, B. K., Sharma, R., Kumar, S., Deka, R. C., Baruah, D. C. & Kalita, E. 2018. Recent trends in the pretreatment of lignocellulosic biomass for value-added products. *Frontiers in Energy Research* 6: 1–19. doi:10.3389/fenrg.2018.00141

Bensah, E. C. & Mensah, M. 2013. Chemical pretreatment methods for the production of cellulosic ethanol: Technologies and innovations. *International Journal of Chemical Engineering* 2013: 1–21. doi:10.1155/2013/719607

Brodeur, G., Yau, E., Badal, K., Collier, J., Ramachandran, K. B. & Ramakrishnan, S. 2011. Chemical and physicochemical pretreatment of lignocellulosic biomass : A review. *Enzyme Research* 2011: 1–17. doi:10.4061/2011/787532

Chieng, B. W., Lee, S. H., Ibrahim, N. A., Then, Y. Y. & Loo, Y. Y. 2017. Isolation and characterization of cellulose nanocrystals from oil palm mesocarp fiber buong. *Polymers* 9(355): 1–11. doi:10.3390/polym9080355

Ching, Y. C. & Ng, T. S. 2014. Effect of preparation conditions on cellulose from oil palm empty fruit bunch fiber. *BioResources* 9(4): 6373–6385. doi:10.15376/biores.9.4.6373-6385

Chowdhury, Z. Z., Chandran, R. R. R., Jahan, A., Khalid, K., Rahman, M. M., Al-Amin, M., Akbarzadeh, O., et al. 2019. Extraction of cellulose nano-whiskers using ionic liquid-assisted ultra-sonication: optimization and mathematical modelling using Box–Behnken design. *Symmetry* 11(1148): 1–20.

Djajadi, D. T., Hansen, A. R., Jensen, A., Thygesen, L. G., Pinelo, M., Meyer, A. S. & Jørgensen, H. 2017. Surface properties correlate to the digestibility of hydrothermally pretreated lignocellulosic Poaceae biomass feedstocks. *Biotechnology for Biofuels* 10(49): 1–15. doi:10.1186/s13068-017-0730-3

Fahma, F., Iwamoto, S., Hori, N., Iwata, T. & Takemura, A. 2010. Isolation, preparation, and characterization of nanofibers from oil palm empty-fruit-bunch (OPEFB). *Cellulose* 17(5): 977–985. doi:10.1007/s10570-010-9436-4

Faizi, M. K., Shahriman, A. B., Majid, M. S. A., Shamsul, B. M. T., Ng, Y. G., Basah, S. N., Cheng, E. M., et al. 2017. An overview of the Oil Palm Empty Fruit Bunch (OPEFB) potential as reinforcing fibre in polymer composite for energy absorption applications. *MATEC Web of Conferences*, hlm. Vol. 01064.

Gonultas, O. & Candan, Z. 2018. Chemical characterization and ftir spectroscopy of thermally compressed eucalyptus wood panels. *Maderas. Ciencia y tecnología* 20(3): 431–442. doi:10.4067/S0718-221X2018005031301

Haan, Mubassir, S., Ho, K. C. & Mohammad, A. W. 2018. A study on membrane technology for surface water treatment : Synthesis , characterization and performance test. *Membrane Water Treatment* 9(2): 69–77. doi:10.12989/mwt.2018.9.2.069

Haan, T. Y., and Mohd Syahmi Hafizi Ghani & Mohammad, A. W. 2018. Physical and Chemical Cleaning for Nanofiltration/ Reverse Osmosis (NF/RO) Membranes in Treatment of Tertiary Palm Oil Mill Effluent (POME) for Water Reclamation. *Jurnal Kejuruteraan* (SI)1(4): 51–58. doi:10.17576/jkukm-2018-si1(4)-07

Haan, Y., Norashiqin, S. & Chun, K. 2020. Sustainable approach to the synthesis of cellulose membrane from oil palm empty fruit bunch for dye wastewater treatment. *Journal of Water Process Engineering* 34(2020): 1–9. doi:10.1016/j.jwpe.2020.101182

Hamzah, N., Tokimatsu, K. & Yoshikawa, K. 2019. Solid fuel from oil palm biomass residues and municipal solid waste by hydrothermal treatment for electrical power generation in Malaysia: A review. *Sustainability* 11(4): 1–23. doi:10.3390/su11041060

Harmsen, P. F. H., Huijgen, W. J. J., López, L. M. B. & Bakker, R. R. C. 2010. Literature Review of Physical and Chemical Pretreatment Processes for Lignocellulosic Biomass. *Biomass*.

Hospodarova, V., Singovszka, E. & Stevulova, N. 2018. Characterization of cellulosic fibers by FTIR spectroscopy for their further implementation to building materials. *American Journal of Analytical Chemistry* 9: 303–310. doi:10.4236/ajac.2018.96023

Huang, W., Wang, E., Chang, J., Wang, P., Yin, Q., Liu, C., Zhu, Q., et al. 2017. Effect of physicochemical pretreatments and enzymatic hydrolysis on corn straw degradation and reducing sugar yield. *BioResources* 12(4): 7002–7015. doi:10.15376/biores.12.4.7002-7015

Ibrahim, Z., Ahmad, M., Aziz, A. A., Ramli, R., Hassan, K. & Alias, A. H. 2019. Properties of chemically treated oil palm empty fruit bunch (EFB) fibres. *Journal of Advanced Research in Fluid Mechanics and Thermal Sciences* 57(1): 57–68.

Isroi, Ishola, M. M., Millati, R., Syamsiah, S., Cahyanto, M. N., Niklasson, C. & Taherzadeh, M. J. 2012. Structural changes of oil palm empty fruit bunch (OPEFB) after fungal and phosphoric acid pretreatment. *Molecules* 17(12): 14995–15012. doi:10.3390/molecules171214995

Khalid, M., Ratnam, C. T., Luqman, C. A., Salmiaton, A., Choong, T. S. Y. & Jalaludin, H. 2009. Thermal and Dynamic Mechanical Behavior of Cellulose- and Oil Palm Empty Fruit Bunch (OPEFB) -Filled Polypropylene Biocomposites. *Polymer-Plastics Technology and Engineering* 48: 1244–1251. doi:10.1080/03602550903282986

Khenblouche, A., Bechki, D., Gouamid, M., Charradi, K., Segni, L., Hadjadj, M. & Boughali, S. 2019. Extraction and characterization of cellulose microfibers from Retama raetam stems. *Polimeros* 29(1): 1–8. doi:10.1590/0104-1428.05218

Kim, D. 2018. Physico-chemical conversion of lignocellulose : Inhibitor effects and detoxification strategies : A mini review. *Molecules* 23(309): 1–21. doi:10.3390/molecules23020309

Li, X., Li, J., Ni, Y. K., Guo, S., Mo, L. & Ni, Y. 2019. Stabilization of Pickering emulsions with cellulose nanofibers derived from oil palm fruit bunch. *Cellulose* 4. doi:10.1007/s10570-019-02803-4

Ling Hii, K., Pin Yeap, S. & Mashitah, M. D. 2014. Utilization of palm pressed pericarp fiber: Pretreatment, optimization and characterization. *Environmental Progress & Sustainable Energy* 33(1): 238–249. doi:10.1002/ep.11757

Martelli-Tosi, M., Assis, O. B. G., Silva, N. C., Esposto, B. S., Martins, M. A. & Tapia-Blácido, D. R. 2017. Chemical treatment and characterization of soybean straw and soybean protein isolate/straw composite films. *Carbohydrate Polymers* 157: 512–520. doi:10.1016/j.carbpol.2016.10.013

Modenbach, A. A. & Nokes, S. E. 2014. Effects of sodium hydroxide pretreatment on structural components of biomass. *Transactions of the ASABE* 57(4): 1187–1198. doi:10.13031/trans.57.10046

Motaung, T. E. & Mtibe, A. 2015. Alkali treatment and cellulose nanowhiskers extracted from maize stalk residues. *Materials Sciences and Applications* 06(11): 1022–1032. doi:10.4236/msa.2015.611102

Nair, G. R. 2017. Role of microwave pre treatment in the extraction of high quality natural fibers. *Journal of Textile Engineering & Fashion Technology Mini* 2(2): 333–335. doi:10.15406/jteft.2017.02.00053

Nazir, M. S., Wahjoedi, B. A., Yussof, A. W. & Abdullah, M. A. 2013. Eco-friendly extraction and characterization of cellulose from oil palm empty fruit bunches. *BioResources* 8(2): 2161–2172. doi:10.15376/biores.8.2.2161-2172

Nordin, I., Hassan, Z. & Razali, N. A. M. 2021. Malaysian Palm Oil Sector Performance in 2020 and Market Opportunities – MPOC. *Malaysian Palm Oil Council*. http://mpoc.org.my/malaysian-palm-oil-sector-performance-in-2020-and-market-opportunities/

Omar, F. N., Mohammed, M. A. P. & Baharuddin, A. S. 2014. Effect of silica bodies on the mechanical behaviour of oil palm empty fruit. *BioResources* 9(4): 7041–7058. doi:10.15376/biores.9.4.7041-7058

Pangsang, N., Rattanapan, U. & Thanapimmetha, A. 2019. Chemical-free fractionation of palm empty fruit bunch and palm fiber by hot-compressed water technique for ethanol production. *Energy Reports* 5: 337–348. doi:10.1016/j.egyr.2019.02.008

Parida, C., Dash, S. K. & Pradhan, C. 2015. FTIR and raman studies of cellulose fibers of luffa cylindrica. *Open Journal of Composite Materials* 05(01): 5–10. doi:10.4236/ojcm.2015.51002

Putro, J. N., Soetaredjo, F. E., Lin, S. Y., Ju, Y. H. & Ismadji, S. 2016. Pretreatment and conversion of lignocellulose biomass into valuable chemicals. *RSC Advances* 6(52): 46834–46852. doi:10.1039/c6ra09851g

Qu, L., Tian, M., Guo, X., Pan, N., Zhang, X. & Zhu, S. 2014. Preparation and properties of natural cellulose fibres from broussonetia papyrifera (L .) Vent . Bast. *Fibres & Textiles in Eastern Europe* 4(106): 24–28.

Rashid, T., Fai, C. & Murugesan, T. 2016. A " fourier transformed infrared " compound study of lignin recovered from a formic acid process. *Procedia Engineering* 148(2016): 1312–1319. doi:10.1016/j.proeng.2016.06.547

Rosli, N. S., Harun, S., Jahim, J. M. & Othaman, R. 2017. Chemical and physical characterization of oil palm empty fruit bunch. *Malaysian Journal of Analytical Sciences* 21(1): 188–196.

Salleh, K. M., Zakaria, S., Sajab, M. S., Gan, S. & Kaco, H. 2019. Superabsorbent hydrogel from oil palm empty fruit bunch cellulose and sodium carboxymethylcellulose. *International Journal of Biological Macromolecules* 131: 50–59. doi:10.1016/j.ijbiomac.2019.03.028

Segal, L., Creely, J. J., A. E. Martin, J. & Conrad, C. M. 1959. Empirical method for estimating the degree of crystallinity of native cellulose using the X-ray diffractometer. *Textile Research Journal* 29(10): 786–794.

Sisak, M. A. A., Daik, R. & Ramli, S. 2015. Characterization of cellulose extracted from oil palm empty fruit bunch. *AIP Conference Proceedings* 1678. doi:10.1063/1.4931295

Sudiyani, Y., Styarini, D. & Triwahyuni, E. 2013. Utilization of biomass waste empty fruit bunch fiber of palm oil for bioethanol production using pilot–scale unit. *Energy Procedia* 32: 31–38. doi:10.1016/j.egypro.2013.05.005

Tanpichai, S., Biswas, S. K., Witayakran, S. & Yano, H. 2019. Water hyacinth: a sustainable lignin-poor cellulose source for the production of cellulose nanofibers. *ACS Sustainable Chemistry and Engineering* 7(23): 18884–18893. doi:10.1021/acssuschemeng.9b04095

Teow, Y., Ming, K. & Mohammad, A. 2018. Synthesis of cellulose hydrogel for copper (II) ions adsorption. *Journal of Environmental Chemical Engineering* 6(4): 4588–4597. doi:10.1016/j.jece.2018.07.010

Thoe, J. M. L., Surugau, N. & Chong, L. H. H. 2019. Application of Oil Palm Empty Fruit Bunch as Adsorbent : A Review. *Transactions on Science and Technology* 6(1): 9–26.

Tsamo, C., Paltahe, A., Fotio, D., Vincent, T. A. & Sales, W. F. 2019. One-, two-, and three-parameter isotherms, kinetics, and thermodynamic evaluation of Co(II) removal from aqueous solution using dead neem leaves. *International Journal of Chemical Engineering* 2019: 1–14. doi:10.1155/2019/6452672

Visakh, P. M. & Morlanes, M. J. M. 2016. Nanomaterials and Nanocomposites_ Zero- to Three-Dimensional Materials and. John Wiley & Sons.

Wang, F. L., Li, S., Sun, Y. X., Han, H. Y., Zhang, B. X., Hu, B. Z., Gao, Y. F., et al. 2017. Ionic liquids as efficient pretreatment solvents for lignocellulosic biomass. *RSC Advances* 7(76): 47990–47998. doi:10.1039/c7ra08110c

Wang, X., Wang, L., Ji, W., Hao, Q., Zhang, G. & Meng, Q. 2019. Characterization of KH-560-modified jute fabric / epoxy laminated composites : Surface structure , and thermal and mechanical properties. *Polymers* 11(769): 1–14.

Wanrosli, W. D., Zainuddin, Z. & Lee, L. K. 2004. Influence of pulping variables on the properties of elaeis guineensis soda pulp as evaluated by response surface methodology. *Wood Science and Technology* 38(3): 191–205. doi:10.1007/s00226-004-0227-7

Yahya, M., Lee, H. V., Abd Hamid, S. B. & Zain, S. K. 2015. Chemical conversion of palm-based lignocellulosic biomass to nano-cellulose: Review. *Polymer Research Journal* 9(4): 1–22. doi:10.1007/s13398-014-0173-7.2

Yang, W., Feng, Y., He, H. & Yang, Z. 2018. Environmentally-friendly extraction of cellulose nanofibers from steam-explosion pretreated sugar beet pulp. *Materials* 11(1160): 1–11. doi:10.3390/ma11071160

Yin, X., Wei, L., Pan, X., Liu, C., Jiang, J. & Wang, K. 2021. The Pretreatment of Lignocelluloses With Green Solvent as Biorefinery Preprocess: A Minor Review. *Frontiers in Plant Science* 12(June). doi:10.3389/fpls.2021.670061

Yu, G., Li, B., Liu, C., Zhang, Y., Wang, H. & Mu, X. 2013. Fractionation of the main components of corn stover by formic acid and enzymatic saccharification of solid residue. *Industrial Crops & Products* 50: 750–757. doi:10.1016/j.indcrop.2013.08.053

Yu, H. T., Chen, B. Y., Li, B. Y., Tseng, M. C., Han, C. C. & Shyu, S. G. 2018. Efficient pretreatment of lignocellulosic biomass with high recovery of solid lignin and fermentable sugars using Fenton reaction in a mixed solvent. *Biotechnology for Biofuels* 11(1): 1–11. doi:10.1186/s13068-018-1288-4

Zhang, K., Pei, Z. & Wang, D. 2016. Organic solvent pretreatment of lignocellulosic biomass for biofuels and biochemicals: A review. *Bioresource Technology* 199: 21–33. doi:10.1016/j.biortech.2015.08.102